



Novel *SCN5A* and *GPD1L* Variants Identified in Two Unrelated Han-Chinese Patients With Clinically Suspected Brugada Syndrome

Meng Yuan^{1†}, Yi Guo^{2†}, Hong Xia³, Hongbo Xu¹, Hao Deng^{1,4,5} and Lamei Yuan^{1,4,5*}

¹ Center for Experimental Medicine, The Third Xiangya Hospital, Central South University, Changsha, China, ² Department of Medical Information, School of Life Sciences, Central South University, Changsha, China, ³ Department of Emergency, The Third Xiangya Hospital, Central South University, Changsha, China, ⁴ Department of Neurology, The Third Xiangya Hospital, Central South University, Changsha, China, ⁵ Disease Genome Research Center, Central South University, Changsha, China

OPEN ACCESS

Edited by:

Christoph Sinning,
University Heart and Vascular Center
Hamburg (UHZ), Germany

Reviewed by:

Douglas A. Marchuk,
Duke University, United States
Oscar Campuzano,
University of Girona, Spain

*Correspondence:

Lamei Yuan
yuanlamei229@163.com

[†]These authors have contributed
equally to this work and share first
authorship

Specialty section:

This article was submitted to
Cardiovascular Genetics and Systems
Medicine,
a section of the journal
Frontiers in Cardiovascular Medicine

Received: 15 August 2021

Accepted: 29 October 2021

Published: 08 December 2021

Citation:

Yuan M, Guo Y, Xia H, Xu H, Deng H
and Yuan L (2021) Novel *SCN5A* and
GPD1L Variants Identified in Two
Unrelated Han-Chinese Patients With
Clinically Suspected Brugada
Syndrome.
Front. Cardiovasc. Med. 8:758903.
doi: 10.3389/fcvm.2021.758903

Brugada syndrome (BrS) is a complexly genetically patterned, rare, malignant, life-threatening arrhythmia disorder. It is autosomal dominant in most cases and characterized by identifiable electrocardiographic patterns, recurrent syncope, nocturnal agonal respiration, and other symptoms, including sudden cardiac death. Over the last 2 decades, a great number of variants have been identified in more than 36 pathogenic or susceptibility genes associated with BrS. The present study used the combined method of whole exome sequencing and Sanger sequencing to identify pathogenic variants in two unrelated Han-Chinese patients with clinically suspected BrS. Minigene splicing assay was used to evaluate the effects of the splicing variant. A novel heterozygous splicing variant c.2437-2A>C in the sodium voltage-gated channel alpha subunit 5 gene (*SCN5A*) and a novel heterozygous missense variant c.161A>T [p.(Asp54Val)] in the glycerol-3-phosphate dehydrogenase 1 like gene (*GPD1L*) were identified in these two patients with BrS-1 and possible BrS-2, respectively. Minigene splicing assay indicated the deletion of 15 and 141 nucleotides in exon 16, resulting in critical amino acid deletions. These findings expand the variant spectrum of *SCN5A* and *GPD1L*, which can be beneficial to genetic counseling and prenatal diagnosis.

Keywords: Brugada syndrome, whole exome sequencing, Han-Chinese patients, minigene splicing assay, novel variants

INTRODUCTION

Brugada syndrome (BrS), first reported in 1992, is a rare, malignant, life-threatening genetic arrhythmia disorder, having no gross structural abnormality (1–4). It has a complex transmission pattern with incomplete penetrance, involving autosomal dominant inheritance in most cases, and autosomal recessive or X-linked inheritance in a few patients (5, 6). BrS planetwide prevalence is estimated to be 1–16 per 10,000, but the true prevalence is difficult to estimate due to the dynamic electrocardiographic pattern and normal sign during the examination, incomplete penetrance, variable expressivity, and problematic diagnosis (7–10). The characteristic BrS electrocardiogram (ECG) can be classified into three types, referring to various ST-segment and T-wave morphologies in the precordial leads (V1–V3). The classic type 1 pattern shows gradually downsloping coved

ST-segment (amplitude ≥ 2 mm) and negative T-wave in more than one lead (V1–V3). In type 2, there is a saddleback ST-segment with an elevation ≥ 2 mm and a positive or biphasic T-wave. The type 3 pattern includes a saddleback or coved pattern with ST-segment elevation < 1 mm. Out of the three patterns in ECG, types 2 and 3 can convert to type 1 under the induction of sodium channel blockers, and only type 1 is diagnostic for BrS (11–13). Patients with BrS can have unexplained recurrent syncope, migraine, seizures, sleep disturbance, nocturnal agonal respiration, self-terminating polymorphic ventricular tachycardia, ventricular fibrillation (VF), inducibility of ventricular tachycardia with programmed electrical stimulation, and atrial arrhythmia, with a type 1 ECG pattern and sudden cardiac death (SCD) in family members (9, 10, 14, 15). Other cardiac conduction disorders, such as atrioventricular block and right bundle branch block (RBBB) can be accompanied, spontaneously occurred, or induced by drug or other factors (5, 8). A BrS diagnostic score system was proposed in 2016 based on an expert consensus statement on the diagnosis and management of inherited primary arrhythmia syndromes in 2013 and guidelines for ventricular arrhythmia management and SCD prevention in 2015, in which the molecular genetic analysis is included for diagnosis confirmation and as a supplement for clinical tests (13, 16, 17). BrS, which often manifests as syncope, has a comparatively higher prevalence in Southeast Asia than those in Europe or the United States (18). It is eight to ten times more common in adult men than women (19). The mean age of the first episode can be 40 years, while BrS may also occur in infancy or early childhood, even leading to sudden infant death syndrome (15).

A variety of genes and variants are associated with BrS. It can be classified into nine types according to the responsible genes in the Online Mendelian Inheritance in Man (OMIM) database. The most common type appears to be BrS-1 (BRGDA1, OMIM 601144), which accounts for 15–30% of cases and is associated with variants in the sodium voltage-gated channel alpha subunit 5 gene (*SCN5A*, OMIM 600163). Other pathogenic variants were reported in a few patients, and variants in the glycerol-3-phosphate dehydrogenase 1 like gene (*GPD1L*, OMIM 611778) were responsible for $< 1\%$ of cases, genetically diagnosed as BrS-2 (BRGDA2, OMIM 611777) (5, 8).

In this study, two novel heterozygous variants, c.2437-2A>C in the *SCN5A* gene, and c.161A>T [p.(Asp54Val)] in the *GPD1L* gene, were identified *via* whole exome sequencing (WES) and Sanger sequencing in two unrelated Han-Chinese patients with clinically suspected BrS. This provides significant human data for improving clinical and genetic diagnosis.

MATERIALS AND METHODS

Subjects and Clinical Evaluations

The participants recruited for the present study were two unrelated Han-Chinese patients from Hunan province in southern China who were suspected to have BrS and an unrelated healthy male without related condition and family history as a control. Professional physical examinations, ECG,

TABLE 1 | Clinical characteristics of two patients.

Case	Patient 1	Patient 2
Sex	Male	Male
Age (years)	42	81
Recurrent syncope	+	–
Nocturnal agonal respiration	–	+
Dizziness	–	+
Palpitation	–	+
Angina	–	+
Migraine	–	–
Seizure	–	–
Sleep disturbance	–	+
Sudden cardiac death in family member (<45 years)	–	+
Brugada electrocardiogram pattern	Type 1	Type 3
Ventricular fibrillation	+	–
Atrioventricular block	First degree	First degree
Right bundle branch block	Incomplete	–

and blood pressure measurements were performed on patients by two experienced cardiologists. Written informed consent was obtained from subjects before participation. The study complied with the Declaration of Helsinki and was approved by the Institutional Review Board of the Third Xiangya Hospital of Central South University.

Exome Capture

Genomic DNA was separated from peripheral blood by the phenol-chloroform method (3). WES was performed for screening the pathogenic variants in two patients by BGI-Shenzhen (Shenzhen, China). One microgram genomic DNA was randomly fragmented using the Covaris technique in which 150–250 bp fragments were selected. DNA fragments were subjected to end-repairing, A-tailing reactions, and adaptor ligation, which were further used for amplification and sequencing. They were further purified and hybridized to the BGI exon array. The captured qualified circular DNA library by rolling circle amplification was sequenced on the BGISEQ-500 sequencing platform (20, 21).

Variants Calling and Validation

The clean reads obtained by trimming and filtering raw reads were aligned with the human reference genome (GRCh37/hg19) by Burrows-Wheeler Aligner (BWA, v0.7.15) (22). Picard (v2.5.0, <http://broadinstitute.github.io/picard/>) removed duplicate reads. Genome Analysis Toolkit (GATK, v3.3.0, <http://www.broadinstitute.org/gatk/guide/best-practices>) tools performed local realignment and base quality score recalibration. HaplotypeCaller in GATK obtained credible single nucleotide polymorphisms (SNPs) and insertions/deletions (InDels) (23). SnpEff software (http://snpeff.sourceforge.net/SnpEff_manual.html) was used for variant annotation and prediction (24). The following databases were used to filter candidate variants, including the Human Gene Mutation Database (HGMD), the Single Nucleotide Polymorphism database (version 154,

dbSNP154), ClinVar, National Heart, Lung and Blood Institute Exome Sequencing Project (ESP6500), Genome Aggregation Database (gnomAD), 1000 Genomes Project (1000G), the China Metabolic Analytics Project (ChinaMAP) database and the in-house BGI exome database (BGI-Shenzhen, Shenzhen, China) with 1,943 Han-Chinese controls (21, 25, 26). Variant pathogenicity was predicted by MutationTaster, Protein Variation Effect Analyzer (PROVEAN), Sorting Intolerant from Tolerant (SIFT), MutationAssessor, Combined Annotation Dependent Depletion (CADD, v1.4), the Berkeley Drosophila Genome Project (BDGP) splice site prediction tool (v0.9), and NetGene2 server (21, 27). Sanger sequencing was performed on the ABI3500 sequencer (Applied Biosystems Inc., Foster City, CA, U.S.A.) for the patients to verify the candidate variants as previously described (28). The following were the paired primer sequences for validating variants in Patient 1 and Patient 2, respectively: 5'-GCTTTCAGGCAGGAGCTAGA-3' and 5'-TGATGGCTAGCACCAGTGTC-3', 5'-CCGCCAAAGTGAGTTTATGT-3', and 5'-TCACCCCAAAGTCTTACCACA-3'. The detected variants were further categorized according to the American College of Medical Genetics and Genomics (ACMG) guidelines for the sequence variant interpretation (27).

Basic Local Alignment Search Tool (BLAST, <https://blast.ncbi.nlm.nih.gov/Blast.cgi>) was used for analyzing protein sequences in nine different species arranged in evolutionary order. The SWISS-MODEL tool (<http://www.swissmodel.expasy.org>) and PyMOL software (version 2.3, Schrödinger, LLC, Portland,

U.S.A.) predicted and visualized wildtype and variant protein structures, respectively (29).

Minigene Splicing Assay

The minigene splicing assay was performed for the splicing variant. The wildtype (WT) and mutant (MT) forms of the minigene constructs composed of two parts, encompassing *SCN5A* exons 15–17, intron 15, and partial intron 16, were amplified from genomic DNA of Patient 1, using the following primer pairs: 5'-AAGCTTGGTACCGAGCTCGGATCCGTCTTCACAGGGATTTCACAGCAGAGA-3' and 5'-CTGTAGGGCATTGGGTGAGTGGACAGATGGTTGATGGA-3', 5'-ACTCACCCAATGCCCTACAGCAGCAGCCCCAGGCTCT-3', and 5'-TTAAACGGGGCCCTCTAGACTCGAGCTGCTTCTGGACTCCTCCTCCGTGCCC-3', and the amplified products were then introduced into the pMini-CopGFP vector (Beijing Hitrobio Biotechnology Co., Ltd., Beijing, China). The vector was double digested at BamHI and XhoI sites. The cloning was achieved by using ClonExpress II One Step Cloning Kit (Vazyme, Nanjing, China). The WT and MT forms of minigene constructs were verified by Sanger sequencing and selected for transfection. Human embryonic kidney (HEK) 293T cells were prepared in Dulbecco's modified Eagle's medium supplemented with 10% fetal bovine serum (HyClone, Logan, Utah, U.S.A.) at 37°C and 5% CO₂. Transfection of minigene constructs was performed using the Lipofectamine 2000 reagent (Invitrogen, Carlsbad, CA, U.S.A.), in accordance with the instructions

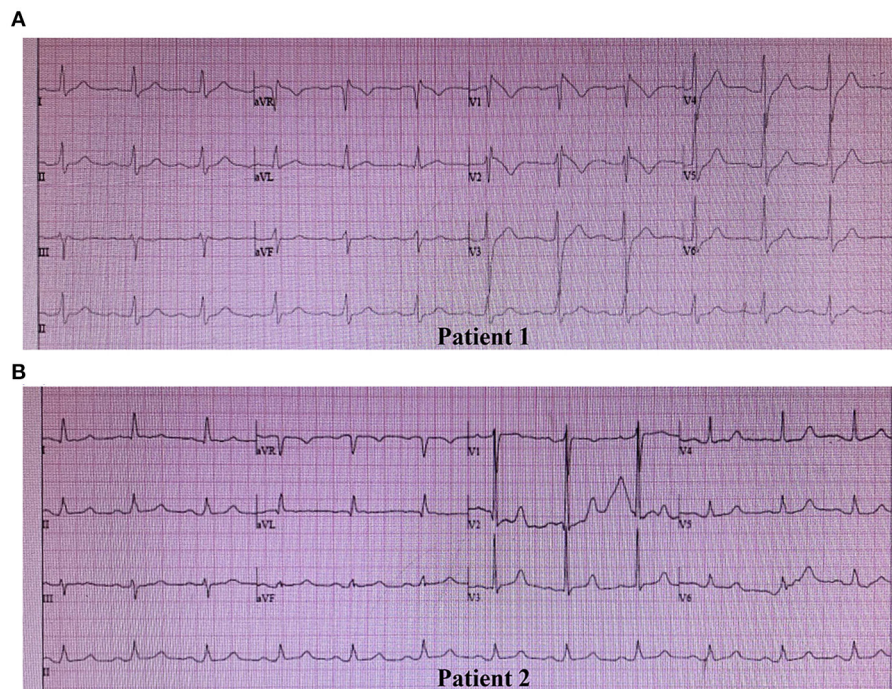


FIGURE 1 | Spontaneous electrocardiogram (ECG) of two patients. **(A)** ECG of Patient 1: Type 1 Brugada pattern displaying a coved-type ST-segment (≥ 2 mm) and negative T wave in V1 and V2, a first-degree atrioventricular block pattern, and an incomplete right bundle branch block. **(B)** ECG of Patient 2: Type 3 Brugada pattern displaying a saddleback ST-segment (< 1 mm) in V2, and a first-degree atrioventricular block pattern.

TABLE 2 | Identification of variants in the patients.

Variant	Variant 1	Variant 2
Gene	<i>SCN5A</i>	<i>GPD1L</i>
Exon	/	2
Intron	15	/
Nucleotide change	c.2437-2A>C	c.161A>T
Amino acid change	p.(Arg814_Leu818del)/ p.(Arg814_Leu860del)	p.(Asp54Val)
Zygoty	Heterozygote	Heterozygote
Variant type	Splicing	Missense
HGMD	No	No
dbSNP154	No	No
ClinVar	No	No
ESP6500	No	No
gnomAD	No	No
1000G	No	No
ChinaMAP database	No	No
In-house BGI exome database	No	No
MutationTaster (probability, prediction)	/	~1, disease causing
PROVEAN (score, prediction)	/	-4.44, deleterious
SIFT (score, prediction)	/	0.033, damaging
MutationAssessor (score, functional impact)	/	2.76, medium
CADD v1.4 (phred-score, prediction)	/	26.6, deleterious
BDGP v0.9	Destroy the acceptor site	/
NetGene2 server	Destroy the acceptor site	/

HGMD, Human Gene Mutation Database; dbSNP154, Single Nucleotide Polymorphism database (version 154); ESP6500, Exome Sequencing Project 6500; gnomAD, Genome Aggregation Database; 1000G, 1000 Genomes Project; ChinaMAP, China Metabolic Analytics Project; PROVEAN, Protein Variation Effect Analyzer; SIFT, Sorting Intolerant from Tolerant; CADD, Combined Annotation Dependent Depletion; BDGP, Berkeley Drosophila Genome Project.

of the manufacturer. At 48-h post-transfection, cells were collected for RNA extraction by using Trizol reagent (Cowan Biotech Co., Ltd., Taizhou, China). Reverse transcription-polymerase chain reaction (RT-PCR) was performed with primers: 5'-GGCTAACTAGAGAACCCACTGCTTA-3' and 5'-GTTTAAACGGCCCTCTAGACTCGA-3', and the products were separated by electrophoresis analysis. Sanger sequencing was applied to identify the isoforms.

RESULTS

Clinical Features

Clinical characteristics and ECG findings of patients are summarized in **Table 1**. Patient 1, a 42-year-old male, was

admitted to the hospital suffering from recurrent syncope (eight times in 8 h), and VF in ECG was detected by the rescue team. ECG suggested a type 1 Brugada pattern, accompanied by a first-degree atrioventricular block and an incomplete RBBB (**Figure 1A**). He had high systolic blood pressure (157/83 mmHg). The condition in Patient 1 was in line with the diagnostic criteria of BRGDA1.

Patient 2 was an 81-year-old male, whose father died of SCD at the age of 44 years. The patient had post-hepatitis cirrhosis and was admitted to the hospital due to gastroesophageal variceal bleeding. His medical history revealed coronary heart disease, grade 3 hypertension (180/100 mmHg), brain atrophy, right renal cysts, chronic cholecystitis, chronic bronchitis, hypoproteinemia, and anemia. He complained of nocturnal agonal respiration, dizziness, palpitation, angina, and sleep disturbance. ECG suggested a type 3 Brugada pattern accompanied by a first-degree atrioventricular block (**Figure 1B**). He was in poor physical shape and passed away shortly after discharge with a highly suspected diagnosis of BrS.

Variant Screening and Bioinformation Analysis

Whole exome sequencing performed on the genomic DNA of Patient 1 produced 115.33 million total effective reads with 99.90% mapped to the human reference sequence, while a total of 153.24 million total effective reads with 99.86% mapped to the human reference sequence were generated with the genomic DNA of Patient 2. For all analyzed genes, the average sequencing depth of the target region was 144.82× for Patient 1 and 192.93× for Patient 2. Of these sequences, 99.24% and 99.57% of the target regions were covered by at least 10×. About 91,330 SNPs and 14,265 InDels were detected in Patient 1. There were 97,957 SNPs and 16,106 InDels detected in Patient 2. These variants were filtered by HGMD, dbSNP154, ClinVar, ESP6500, gnomAD, 1000G, ChinaMAP database, and in-house BGI exome database to assess possible pathogenic variants in the patients. MutationTaster, PROVEAN, SIFT, MutationAssessor, CADD, BDGP splice site prediction tool, and NetGene2 server predicted the potential variants to be deleterious (**Table 2**). After screening the above databases and analyzing all known BrS-associated genes, only two novel and damaging heterozygous variants, c.2437-2A>C in the *SCN5A* gene (NG_008934.1, NM_001099404.1) and c.161A>T [p.(Asp54Val)] in the *GPD1L* gene (NM_015141.3, NP_055956.1), were considered as potential disease-causing variants in Patient 1 and Patient 2, respectively. Sanger sequencing confirmed these variants (**Figure 2**). The c.2437-2A>C variant was classified as “pathogenic” (PVS1 + PM2 + PP3), and the c.161A>T variant was classified as “likely pathogenic” (PM1 + PM2 + PP2 + PP3), following the ACMG guidelines.

Basic Local Alignment Search Tool comparison of protein sequences from human to chicken revealed that p.Asp54 was highly conserved in GPD1L protein (**Figure 3A**). A structural model showed the conformational alteration of aspartic acid (Asp-54) into valine (Val-54), further confirming the possible pathogenicity of the variant (**Figure 3B**).

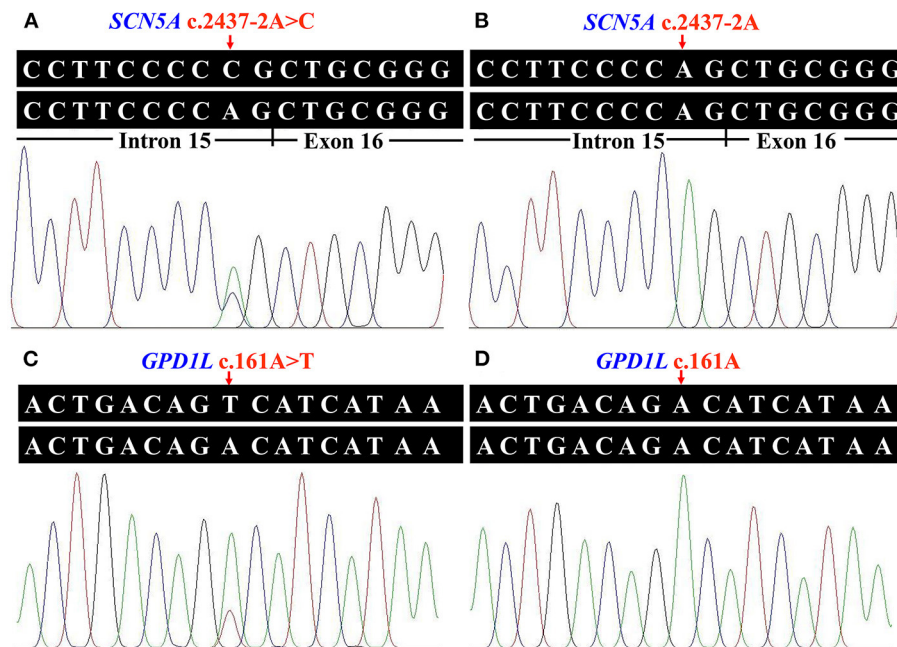
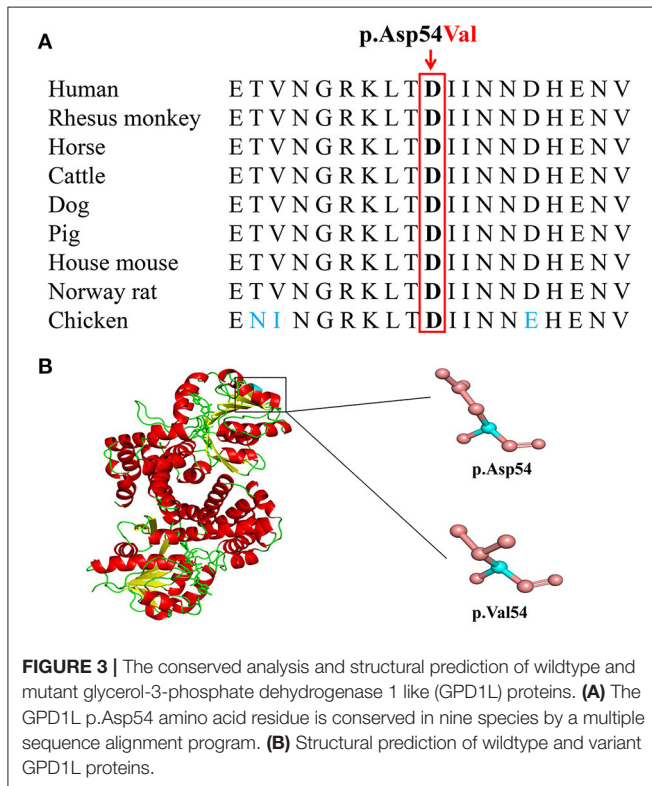


FIGURE 2 | Identified variants of the sodium voltage-gated channel alpha subunit 5 gene (*SCN5A*) and the glycerol-3-phosphate dehydrogenase 1 like gene (*GPD1L*) in the two patients. **(A)** Heterozygous transversion (c.2437-2A>C) at the splice acceptor site of *SCN5A* intron 15 in Patient 1. **(B)** The normal *SCN5A* sequence of an unaffected individual. **(C)** The *GPD1L* sequence with heterozygous c.161A>T [p.(Asp54Val)] variant in Patient 2. **(D)** The normal *GPD1L* sequence of an unaffected individual.

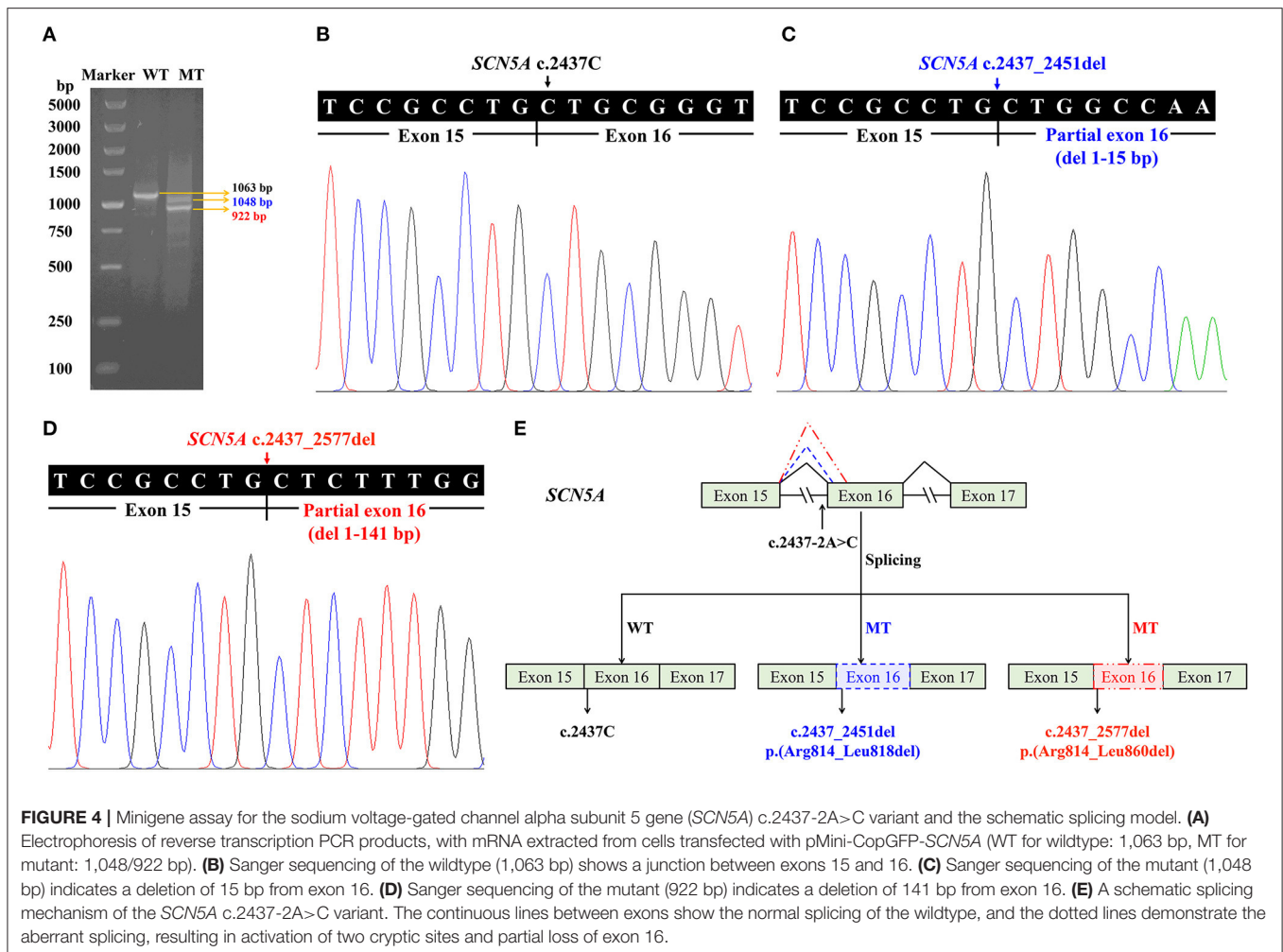


Splicing Analysis of *SCN5A* c.2437-2A>C in the Minigene

Minigene assay and RT-PCR analysis were performed to identify the abnormal splicing. Electrophoresis analysis of RT-PCR products showed a single band for WT and two shorter bands for MT (**Figure 4A**). Sanger sequencing indicated normal splicing in exons 15 and 16 for WT (**Figure 4B**), and partial loss of exon 16 for MT, including the deletion of the first 15 nucleotides (c.2437_2451del) and 141 nucleotides from exon 16 (c.2437_2577del) (**Figures 4C,D**). It indicated that the *SCN5A* c.2437-2A>C variant can abolish the intron 15 canonical acceptor splice site and lead to activation of two cryptic sites in exon 16, predicted to cause in-frame deletions, p.(Arg814_Leu818del) and p.(Arg814_Leu860del) (**Figure 4E**).

DISCUSSION

Brugada syndrome seems to have a poor genotype-phenotype correlation, with obvious genetic and phenotypic heterogeneity (30, 31). Incomplete penetrance and even asymptomatic gene carriers have been commonly reported (30, 32). Since *SCN5A* was reported as a causative gene of BrS in 1998, a great number of variants have been identified in more than 36 pathogenic or susceptibility genes associated with BrS in the past 2 decades (**Figure 5**) (33–35).



In the present study, c.2437-2A>C in the *SCN5A* gene was prosecuted as the pathogenic variant for Patient 1 with BRGDA1, and c.161A>T [p.(Asp54Val)] in the *GPD1L* gene was considered as the potential pathogenic variant in Patient 2 with possible BRGDA2 lacking an available drug challenge test. Currently, more than 950 *SCN5A* gene variants have been reported, and more than 360 variants have been recorded as responsible for BRGDA1 (<http://www.hgmd.cf.ac.uk/ac/index.php>, <http://www.lovd.nl/3.0/home>). The single nucleotide substitution affecting splicing accounted for 6% of BRGDA1 (Figure 6A). However, only three substitutions in the *GPD1L* gene, c.370A>G (p.Ile124Val), c.565C>T (p.Arg189*), and c.839C>T (p.Ala280Val), have been found to be related to BRGDA2 (Figure 6B) (36). The c.2437-2A>C variant was located at the splice acceptor site of intron 15 in the *SCN5A* gene, and this transversion was predicted to destroy the splice acceptor site by the BDGP splice site prediction tool and NetGene2 server. *In silico* programs (MutationTaster, PROVEAN, SIFT, MutationAssessor, and CADD) predicted that the c.161A>T transversion in the *GPD1L* gene would be deleterious. The conclusion that these variants were pathogenic is further

supported by their absence in public variant databases and the 1,943 Han-Chinese controls of the in-house BGI exome database.

Sodium voltage-gated channel alpha subunit 5 gene, located at chromosome 3p22.2, has 28 exons and encodes the α -subunit of the cardiac voltage-gated sodium channel ($\text{Na}_v1.5$) protein, which contains 2016-amino acid (15, 37, 38). The highly cardiac-specific $\text{Na}_v1.5$ is located in T-tubule membranes and intercalated discs in cardiomyocytes (<http://biogps.org>) (39, 40). It consists of four putative homologous repetitive transmembrane domains: DI (113–420 amino acids), DII (699–969 amino acids), DIII (1,187–1,501 amino acids), and DIV (1,510–1,807 amino acids). Each domain contains six transmembrane segments (S1–S6), including five hydrophobic regions (S1–S3, S5, and S6) and a positively charged segment (S4), probably acting as a voltage sensor (<https://www.uniprot.org/uniprot/>, Figure 6A) (33). The $\text{Na}_v1.5$ channel is able to conduct a depolarized sodium inward current, forming a rapidly rising action potential in an activated process, which plays an important role in cardiomyocyte excitability and normal electrical pulse conduction (38, 41).

The c.2437-2A>C variant in the *SCN5A* gene is located in the 3' splice junctions at the boundary between intron 15 and

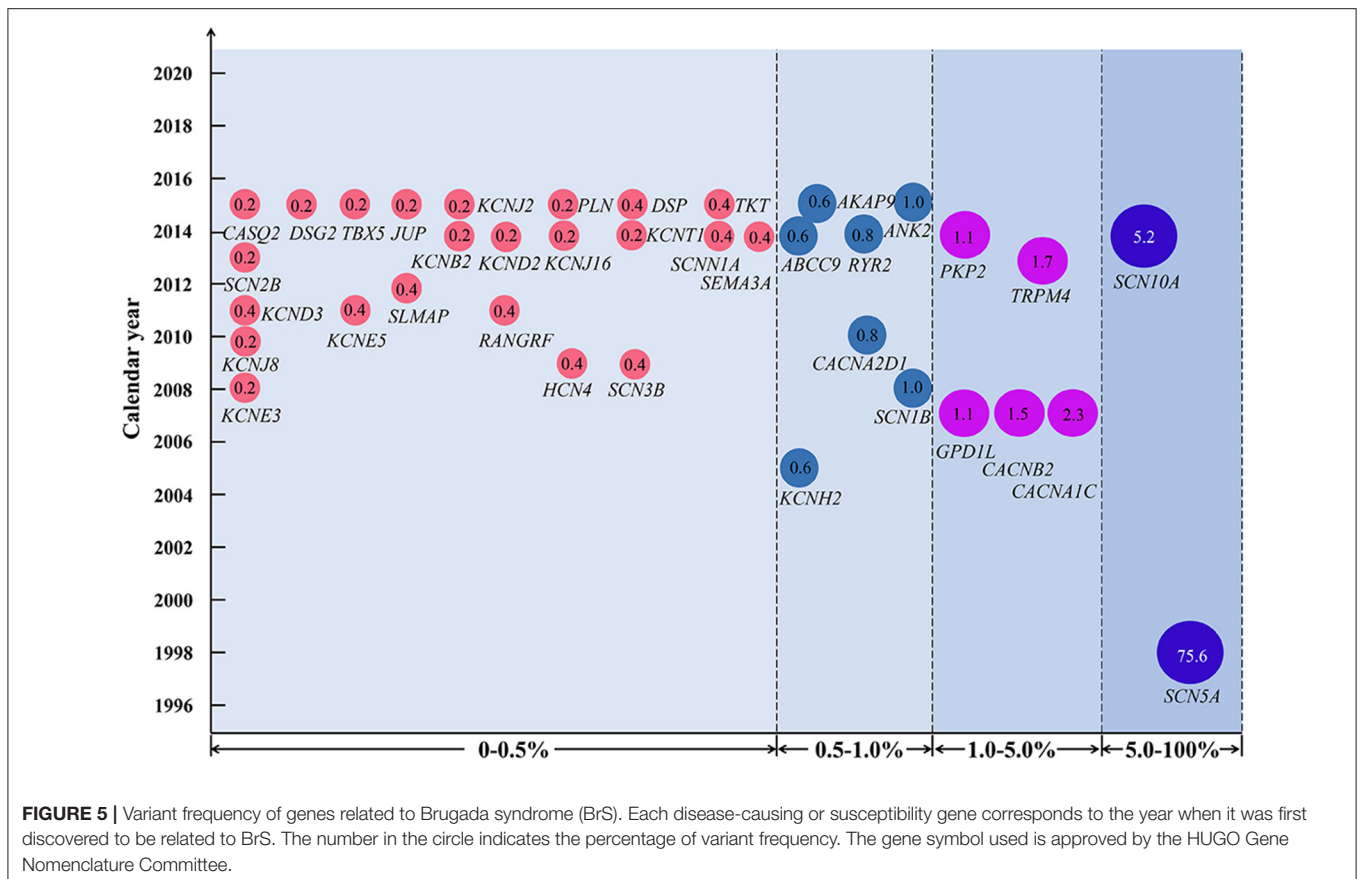


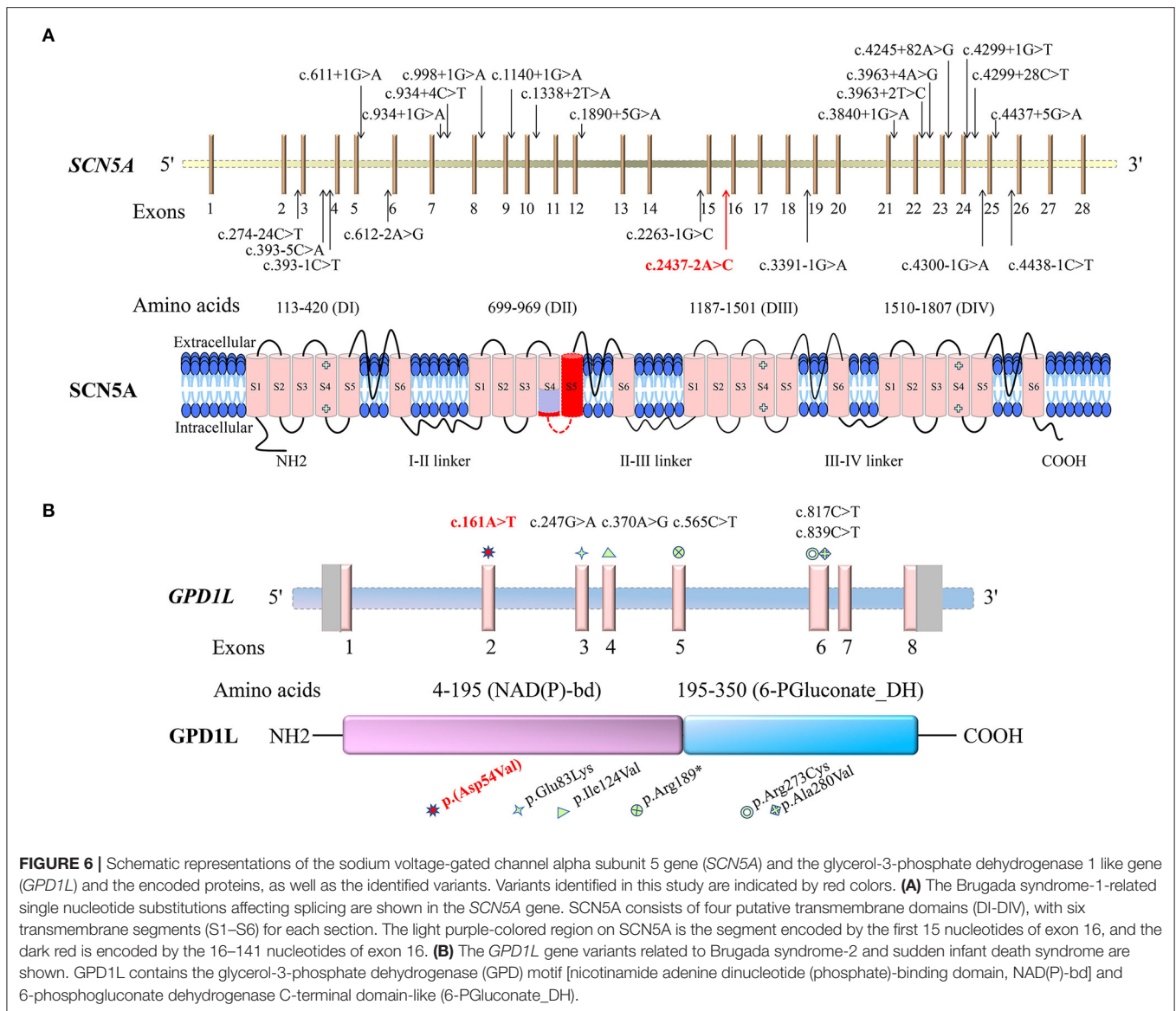
FIGURE 5 | Variant frequency of genes related to Brugada syndrome (BrS). Each disease-causing or susceptibility gene corresponds to the year when it was first discovered to be related to BrS. The number in the circle indicates the percentage of variant frequency. The gene symbol used is approved by the HUGO Gene Nomenclature Committee.

exon 16, where canonical AG dinucleotides appear. Minigene assay showed that the variant destroyed the canonical acceptor site and activated the cryptic splice sites in exon 16, predicted to cause in-frame deletion of 5 [p.(Arg814_Leu818del)] and 47 amino acids [p.(Arg814_Leu860del)], corresponding to the transmembrane segments of S4 and S5 in DII of $\text{Na}_v1.5$ protein, which is critical to the voltage-sensor function. Previous studies showed that BrS-related *SCN5A* variants could lead to loss of function of the sodium channel mediated by haploinsufficiency (42, 43), or the related variant channels exert a dominant-negative effect on the WT channels (41). The mechanism of BrS caused by the c.2437-2A>C variant in Patient 1 may be similar to the pathogenesis of variants in nearby residues of the same domain, which is related to loss of function of the sodium channel (44).

Heterozygous *SCN5A*-p.Arg367His patient-specific-induced pluripotent stem cell-derived cardiomyocytes had decreased sodium inward current density, changed voltage-dependent curves in activation and inactivation, and accelerated recovery from inactivation (45). Transgenic zebrafish with the cardiac expression of human *SCN5A* p.Asp1275Asn variant revealed some clinical manifestations related to BrS, such as conduction disorders and early death (46). *Scn5a*^{-/-} mice had severe defects to embryonic lethality, while *Scn5a*^{+/-} mice were viable and showed decreased sodium channel density and slowed conduction (47).

Glycerol-3-phosphate dehydrogenase 1 like gene, located at chromosome 3p22.3, a position near to *SCN5A*, includes eight exons and expresses a 351-amino acid membrane-associated protein with a molecular mass of 40 kD. The protein is highly expressed in the heart (34, 48). It contains N-terminal glycerol-3-phosphate dehydrogenase (GPD) motif (nicotinamide adenine dinucleotide (phosphate)-binding domain, 4–195 amino acids) and 6-phosphogluconate dehydrogenase C-terminal domain-like (195–350 amino acids), in which amino acids 22–28 are highly homologous to amino acids 830–836 in the transmembrane domain of $\text{Na}_v1.5$ (Figure 6B) (34, 36). As a member of the GPD family, *GPD1L* has an 84% amino acid homology to *GPD1* and is involved in glucose and nicotinamide adenine dinucleotide-dependent energy metabolism, mammalian respiratory chain, and glycerophosphate shuttle (49, 50). It may have a cardiac-specific physiological function and may be coupled with $\text{Na}_v1.5$, which can link the myocardial metabolic state to cellular excitability by modulating sodium current density, responsible for cardiac conduction disorder (48).

The c.161A>T variant in the *GPD1L* gene of exon 2 may lead to an aspartic acid-to-valine substitution, p.(Asp54Val), changing from a negatively charged acidic hydrophilic amino acid residue to a neutral hydrophobic amino acid residue, which may impact the tertiary structure or function. Aspartic acid at position 54 was conserved in different species by a multiple sequence alignment program, supporting that the



amino acid change may lead to protein function changes. The variant p.(Asp54Val), located in the nicotinamide adenine dinucleotide (phosphate)-binding domain, may have the same pathogenic mechanism as the sudden infant death syndrome-related p.Glu83Lys variant in the same domain and the BrS-related p.Ala280Val variant outside the domain. Both variants have been shown to result in the decrease of enzyme activity and the increase of substrate glycerol-3-phosphate, which further leads to increased $\text{Na}_v1.5$ phosphorylation *via* the *GPD1L*-dependent pathway, significantly decreasing the sodium current density and leading to the conduction disorder (48).

CONCLUSIONS

A novel splicing variant c.2437-2A>C in the *SCN5A* gene and a novel missense variant c.161A>T [p.(Asp54Val)] in the *GPD1L*

gene were identified in two unrelated Han-Chinese patients with BRGDA1 and possible BRGDA2, respectively. These findings expand the variant spectrum of *SCN5A* and *GPD1L*, which can be beneficial to genetic counseling and prenatal diagnosis. Universal, affordable, and efficient WES has the potential to uncover unsuspected rare or common variants for heterogeneous disorders, like BrS (51–53). The combined strategy of WES and Sanger sequencing can facilitate timely diagnoses and optimal care for those with clinically suspected BrS, presenting weak disease evidence. The limitation of this study is that the influence of oligogenic inheritance, background genotype, and environmental factors on BrS cannot be excluded. Due to the privacy concerns of Patient 1 and the death of Patient 2 without an offspring, co-segregation analysis was limited, and identification of the same variants in more confirmed patients will help to further support the pathogenicity of c.2437-2A>C in

the SCN5A gene and determine the pathogenicity of c.161A>T in the GPD1L gene. Further functional studies *in vitro* and/or *in vivo* will help to elucidate the potential pathogenic mechanism of BrS.

DATA AVAILABILITY STATEMENT

According to national legislation/guidelines, specifically the Administrative Regulations of the People's Republic of China on Human Genetic Resources (http://www.gov.cn/zhengce/content/2019-06/10/content_5398829.htm, http://english.www.gov.cn/policies/latest_releases/2019/06/10/content_281476708945462.htm), no additional raw data is available at this time. Data of this project can be accessed after an approval application to the China National GeneBank (CNGB, <https://db.cngb.org/cnsa/>). Please refer to <https://db.cngb.org/>, or email: CNGBdb@cngb.org for detailed application guidance. The accession code CNP0002245 should be included in the application.

ETHICS STATEMENT

The studies involving human participants were reviewed and approved by the Institutional Review Board of the Third Xiangya Hospital of Central South University. The patients/participants provided their written informed consent to participate in this study. Written informed consent was obtained from the participants or their legal guardian/next of kin for the publication of any

REFERENCES

- Duffett SA, Roberts JD. Brugada syndrome: evolving insights and emerging treatment strategies. *J Innov Card Rhythm Manag.* (2017) 8:2613–22. doi: 10.19102/icrm.2017.080205
- Schwartz PJ, Ackerman MJ, Antzelevitch C, Bezzina CR, Borggrefe M, Cuneo BF, et al. Inherited cardiac arrhythmias. *Nat Rev Dis Primers.* (2020) 6:58. doi: 10.1038/s41572-020-0188-7
- Probst V, Wilde AAM, Barc J, Sacher F, Babuty D, Mabo P, et al. SCN5A mutations and the role of genetic background in the pathophysiology of Brugada syndrome. *Circ Cardiovasc Genet.* (2009) 2:552–7. doi: 10.1161/CIRCGENETICS.109.853374
- Brugada P, Brugada J. Right bundle branch block, persistent ST segment elevation and sudden cardiac death: a distinct clinical and electrocardiographic syndrome. A multicenter report. *J Am Coll Cardiol.* (1992) 20:1391–6. doi: 10.1016/0735-1097(92)90253-J
- Brugada R, Campuzano O, Sarquella-Brugada G, Brugada P, Brugada J, Hong K. *Brugada Syndrome*. Seattle, WA: University of Washington (2005).
- Janin A, Bessière F, Georgescu T, Chanavat V, Chevalier P, Millat G. TRPM4 mutations to cause autosomal recessive and not autosomal dominant Brugada type 1 syndrome. *Eur J Med Genet.* (2019) 62:103527. doi: 10.1016/j.ejmg.2018.08.008
- Sacilotto L, Scanavacca MI, Olivetti N, Lemes C, Pessente GD, Wulkan F, et al. Low rate of life-threatening events and limitations in predicting invasive and noninvasive markers of symptoms in a cohort of type 1 Brugada syndrome patients: data and insights from the GenBra registry. *J Cardiovasc Electrophysiol.* (2020) 31:2920–8. doi: 10.1111/jce.14732

potentially identifiable images or data included in this article.

AUTHOR CONTRIBUTIONS

MY, YG, and LY conceived and designed this study. YG, HXia, and LY collected the patient samples and clinical data. MY, YG, and HXu performed the experiments. MY, HD, and LY analyzed the data. MY, YG, HD, and LY wrote the manuscript. The final version of the manuscript was read and approved by all authors.

FUNDING

This study was supported by the National Natural Science Foundation of China (Grant Nos. 81800219 and 81873686), Natural Science Foundation of Hunan Province (Grant Nos. 2019JJ50927, 2020JJ3057, and 2020JJ4830), Scientific Research Project of Health Commission of Hunan Province, China (Grant No. B2019174), the Wisdom Accumulation and Talent Cultivation Project of the Third Xiangya Hospital of Central South University (Grant No. YX202109), and Distinguished Professor of the Lotus Scholars Award Program of Hunan Province, China.

ACKNOWLEDGMENTS

We extend our greatest gratitude to patients, their families, physicians, and researchers for their cooperation and contribution.

- Monasky MM, Micaglio E, Ciconte G, Pappone C. Brugada syndrome: oligogenic or mendelian disease? *Int J Mol Sci.* (2020) 21:1687. doi: 10.3390/ijms21051687
- Hasdemir C, Gokcay F, Orman MN, Kocabas U, Payzin S, Sahin H, et al. Recognition and clinical implications of high prevalence of migraine in patients with Brugada syndrome and drug-induced type 1 Brugada pattern. *J Cardiovasc Electrophysiol.* (2020) 31:3311–7. doi: 10.1111/jce.14778
- Sarquella-Brugada G, Campuzano O, Arbelo E, Brugada J, Brugada R. Brugada syndrome: clinical and genetic findings. *Genet Med.* (2016) 18:3–12. doi: 10.1038/gim.2015.35
- Roomi SS, Ullah W, Abbas H, Abdullah H, Talib U, Figueredo V. Brugada syndrome unmasked by fever: a comprehensive review of literature. *J Community Hosp Intern Med Perspect.* (2020) 10:224–8. doi: 10.1080/20009666.2020.1767278
- Flamée P, Varnavas V, Dewals W, Carvalho H, Cools W, Bhutia JT, et al. Electrocardiographic effects of propofol versus etomidate in patients with Brugada syndrome. *Anesthesiology.* (2020) 132:440–51. doi: 10.1097/ALN.0000000000003030
- Antzelevitch C, Yan GX, Ackerman MJ, Borggrefe M, Corrado D, Guo J, et al. J-Wave syndromes expert consensus conference report: emerging concepts and gaps in knowledge. *J Arrhythm.* (2016) 32:315–39. doi: 10.1016/j.joa.2016.07.002
- Bordachar P, Reuter S, Garrigue S, Cai X, Hocini M, Jaïs P, et al. Incidence, clinical implications and prognosis of atrial arrhythmias in Brugada syndrome. *Eur Heart J.* (2004) 25:879–84. doi: 10.1016/j.ehj.2004.01.004
- Hedley PL, Jørgensen B, Schlamowitz S, Moolman-Smook J, Kanters JK, Corfield VA, et al. The genetic basis of Brugada syndrome: a mutation update. *Hum Mutat.* (2009) 30:1256–66. doi: 10.1002/humu.21066
- Priori SG, Wilde AA, Horie M, Cho Y, Behr ER, Berul C, et al. HRS/EHRA/APHRS expert consensus statement on the diagnosis and

- management of patients with inherited primary arrhythmia syndromes: document endorsed by HRS, EHRA, and APhRS in May 2013 and by ACCF, AHA, PACES, and AEP in June 2013. *Heart Rhythm*. (2013) 10:1932–63. doi: 10.1016/j.hrthm.2013.05.014
17. Priori SG, Blomström-Lundqvist C. 2015 European Society of Cardiology Guidelines for the management of patients with ventricular arrhythmias and the prevention of sudden cardiac death summarized by co-chairs. *Eur Heart J*. (2015) 36:2757–9. doi: 10.1093/eurheartj/ehv445
 18. Antzelevitch C, Brugada P, Borggrefe M, Brugada J, Brugada R, Corrado D, et al. Brugada syndrome: report of the second consensus conference. *Heart Rhythm*. (2005) 2:429–40. doi: 10.1016/j.hrthm.2005.01.005
 19. Malik BR, Ali Rudwan AM, Abdelghani MS, Mohsen M, Khan SHA, Aljefairi N, et al. Brugada syndrome: clinical features, risk stratification, and management. *Heart Views*. (2020) 21:88–96. doi: 10.4103/HEARTVIEWS.HEARTVIEWS_44_20
 20. Huang J, Liang X, Xuan Y, Geng C, Li Y, Lu H, et al. A reference human genome dataset of the BGISEQ-500 sequencer. *GigaScience*. (2017) 6:1–9. doi: 10.1093/gigascience/gix024
 21. Fan K, Zhu H, Xu H, Mao P, Yuan L, Deng H. The identification of a transthyretin variant p.D38G in a Chinese family with early-onset leptomeningeal amyloidosis. *J Neurol*. (2019) 266:232–41. doi: 10.1007/s00415-018-9125-z
 22. Li H, Durbin R. Fast and accurate long-read alignment with Burrows-Wheeler transform. *Bioinformatics*. (2010) 26:589–95. doi: 10.1093/bioinformatics/btp698
 23. Summa SD, Malerba G, Pinto R, Mori A, Mijatovic V, Tommasi S. GATK hard filtering: tunable parameters to improve variant calling for next generation sequencing targeted gene panel data. *BMC Bioinformatics*. (2017) 18:119. doi: 10.1186/s12859-017-1537-8
 24. Cingolani P, Platts A, Wang LL, Coon M, Nguyen T, Wang L, et al. A program for annotating and predicting the effects of single nucleotide polymorphisms, SnpEff: SNPs in the genome of drosophila melanogaster strain w1118; iso-2; iso-3. *Fly*. (2012) 6:80–92. doi: 10.4161/fly.19695
 25. Cao Y, Li L, Xu M, Feng Z, Sun X, Lu J, et al. The ChinaMAP analytics of deep whole genome sequences in 10,588 individuals. *Cell Res*. (2020) 30:717–31. doi: 10.1038/s41422-020-0322-9
 26. Deng S, Wu S, Xia H, Xiong W, Deng X, Liao J, et al. Identification of a frame shift mutation in the CCDC151 gene in a Han-Chinese family with Kartagener syndrome. *Biosci Rep*. (2020) 40:BSR20192510. doi: 10.1042/BSR20192510
 27. Richards S, Aziz N, Bale S, Bick D, Das S, Gastier-Foster J, et al. Standards and guidelines for the interpretation of sequence variants: a joint consensus recommendation of the American College of Medical Genetics and Genomics and the Association for Molecular Pathology. *Genet Med*. (2015) 17:405–24. doi: 10.1038/gim.2015.30
 28. He D, Hu P, Deng X, Song Z, Yuan L, Yuan X, et al. Genetic analysis of the RIC3 gene in Han Chinese patients with Parkinson's disease. *Neurosci Lett*. (2017) 653:351–4. doi: 10.1016/j.neulet.2017.06.007
 29. Xiang Q, Cao Y, Xu H, Guo Y, Yang Z, Xu L, et al. Identification of novel pathogenic ABCA4 variants in a Han Chinese family with Stargardt disease. *Biosci Rep*. (2019) 39:BSR20180872. doi: 10.1042/BSR20180872
 30. Li KHC, Lee S, Yin CY, Liu T, Ngarmukos T, Conte G, et al. Brugada syndrome: a comprehensive review of pathophysiological mechanisms and risk stratification strategies. *Int J Cardiol Heart Vasc*. (2020) 26:100468. doi: 10.1016/j.ijcha.2020.100468
 31. Verkerk AO, Amin AS, Remme CA. Disease modifiers of inherited SCN5A channelopathy. *Front Cardiovasc Med*. (2018) 5:137. doi: 10.3389/fcvm.2018.00137
 32. Gaborit N, Wichter T, Varro A, Szuts V, Lamirault G, Eckardt L, et al. Transcriptional profiling of ion channel genes in Brugada syndrome and other right ventricular arrhythmogenic diseases. *Eur Heart J*. (2009) 30:487–96. doi: 10.1093/eurheartj/ehn520
 33. Chen Q, Kirsch GE, Zhang D, Brugada R, Brugada J, Brugada P, et al. Genetic basis and molecular mechanism for idiopathic ventricular fibrillation. *Nature*. (1998) 392:293–6. doi: 10.1038/32675
 34. London B, Michalec M, Mehdiet H, Zhu X, Kerchner L, Sanyal S, et al. Mutation in glycerol-3-phosphate dehydrogenase 1 like gene (GPD1-L) decreases cardiac Na⁺ current and causes inherited arrhythmias. *Circulation*. (2007) 116:2260–8. doi: 10.1161/CIRCULATIONAHA.107.703330
 35. Campuzano O, Sarquella-Brugada G, Cesar S, Arbelo E, Brugada J, Brugada R. Update on genetic basis of Brugada syndrome: monogenic, polygenic or oligogenic? *Int J Mol Sci*. (2020) 21:7155. doi: 10.3390/ijms21197155
 36. Huang H, Chen YQ, Fan LL, Guo S, Li JJ, Jin JY, et al. Whole-exome sequencing identifies a novel mutation of GPD1L (R189X) associated with familial conduction disease and sudden death. *J Cell Mol Med*. (2018) 22:1350–4. doi: 10.1111/jcmm.13409
 37. Shah S, Nelson CP, Gaunt TR, van der Harst P, Barnes T, Braund PS, et al. Four genetic loci influencing electrocardiographic indices of left ventricular hypertrophy. *Circ Cardiovasc Genet*. (2011) 4:626–35. doi: 10.1161/CIRCGENETICS.111.960203
 38. Wang Y, Du Y, Luo L, Hu P, Yang G, Li T, et al. Alterations of Nedd4-2-binding capacity in PY-motif of Nav_v1.5 channel underlie long QT syndrome and Brugada syndrome. *Acta Physiol*. (2020) 229:e13438. doi: 10.1111/apha.13438
 39. Wu C, Jin X, Tsung G, Afrasiabi C, Su AI. BioGPS: building your own mash-up of gene annotations and expression profiles. *Nucleic Acids Res*. (2016) 44:D313–6. doi: 10.1093/nar/gkv1104
 40. Mohler PJ, Rivolta I, Napolitano C, LeMaillet G, Lambert S, Priori SG, et al. Nav1.5 E1053K mutation causing Brugada syndrome blocks binding to ankyrin-G and expression of Nav1.5 on the surface of cardiomyocytes. *Proc Natl Acad Sci USA*. (2004) 101:17533–8. doi: 10.1073/pnas.0403711101
 41. Wang Z, Vermij SH, Sottas V, Shestak A, Ross-Kaschitzka D, Zaklyazminskaya EV, et al. Calmodulin binds to the N-terminal domain of the cardiac sodium channel Nav_v1.5. *Channels*. (2020) 14:268–86. doi: 10.1080/19336950.2020.1805999
 42. Finlay M, Bhar-Amato J, Ng KE, Santos D, Orini M, Vyas V, et al. Autonomic modulation of the electrical substrate in mice haploinsufficient for cardiac sodium channels: a model of the Brugada syndrome. *Am J Physiol Cell Physiol*. (2019) 317:C576–83. doi: 10.1152/ajpcell.00028.2019
 43. Jeevaratnam K, Guzadhur L, Goh YM, Grace AA, Huang CL. Sodium channel haploinsufficiency and structural change in ventricular arrhythmogenesis. *Acta Physiol*. (2016) 216:186–202. doi: 10.1111/apha.12577
 44. Kinoshita K, Takahashi H, Hata Y, Nishide K, Kato M, Fujita H, et al. SCN5A (K817E), a novel Brugada syndrome-associated mutation that alters the activation gating of Nav1.5 channel. *Heart Rhythm*. (2016) 13:1113–20. doi: 10.1016/j.hrthm.2016.01.008
 45. Selga E, Sendfeld F, Martinez-Moreno R, Medine CN, Tura-Ceide O, Wilmot SI, et al. Sodium channel current loss of function in induced pluripotent stem cell-derived cardiomyocytes from a Brugada syndrome patient. *J Mol Cell Cardiol*. (2018) 114:10–9. doi: 10.1016/j.yjmcc.2017.10.002
 46. Huttner IG, Trivedi G, Jacoby A, Mann SA, Vandenberg JJ, Fatkin D. A transgenic zebrafish model of a human cardiac sodium channel mutation exhibits bradycardia, conduction-system abnormalities and early death. *J Mol Cell Cardiol*. (2013) 61:123–32. doi: 10.1016/j.yjmcc.2013.06.005
 47. Papadatos GA, Wallerstein PMR, Head CEG, Ratcliff R, Brady PA, Benndorf K, et al. Slowed conduction and ventricular tachycardia after targeted disruption of the cardiac sodium channel gene Scn5a. *Proc Natl Acad Sci USA*. (2002) 99:6210–5. doi: 10.1073/pnas.082121299
 48. Valdivia CR, Ueda K, Ackerman MJ, Makielski JC. GPD1L links redox state to cardiac excitability by PKC-dependent phosphorylation of the sodium channel SCN5A. *Am J Physiol Heart Circ Physiol*. (2009) 297:H1446–52. doi: 10.1152/ajpheart.00513.2009
 49. Liu M, Sanyal S, Gao G, Gurung IS, Zhu X, Gaconnet G, et al. Cardiac Na⁺ current regulation by pyridine nucleotides. *Circ Res*. (2009) 105:737–45. doi: 10.1161/CIRCRESAHA.109.197277
 50. Denti F, Paludan-Müller C, Olesen SP, Haunso S, Svendsen JH, Olesen MS, et al. Functional consequences of genetic variation in sodium channel modifiers in early onset lone atrial fibrillation. *Per Med*. (2018) 15:93–102. doi: 10.2217/pme-2017-0076

51. Stenton SL, Prokisch H. Advancing genomic approaches to the molecular diagnosis of mitochondrial disease. *Essays Biochem.* (2018) 62:399–408. doi: 10.1042/EBC20170110
52. Huang X, Yuan L, Xu H, Zheng W, Cao Y, Yi J, et al. Identification of a novel mutation in the *ABCA4* gene in a Chinese family with retinitis pigmentosa using exome sequencing. *Biosci Rep.* (2018) 38:BSR20171300. doi: 10.1042/BSR20171300
53. Refaat MM, Hotait M, London B. Genetics of sudden cardiac death. *Curr Cardiol Rep.* (2015) 17:606. doi: 10.1007/s11886-015-0606-8

Conflict of Interest: The authors declare that the research was conducted in the absence of any commercial or financial relationships that could be construed as a potential conflict of interest.

Publisher's Note: All claims expressed in this article are solely those of the authors and do not necessarily represent those of their affiliated organizations, or those of the publisher, the editors and the reviewers. Any product that may be evaluated in this article, or claim that may be made by its manufacturer, is not guaranteed or endorsed by the publisher.

Copyright © 2021 Yuan, Guo, Xia, Xu, Deng and Yuan. This is an open-access article distributed under the terms of the Creative Commons Attribution License (CC BY). The use, distribution or reproduction in other forums is permitted, provided the original author(s) and the copyright owner(s) are credited and that the original publication in this journal is cited, in accordance with accepted academic practice. No use, distribution or reproduction is permitted which does not comply with these terms.